

DOI: [10.29026/oes.2022.210014](https://doi.org/10.29026/oes.2022.210014)

# Terahertz metasurface zone plates with arbitrary polarizations to a fixed polarization conversion

Zhen Yue<sup>1†</sup>, Jitao Li<sup>1†</sup>, Jie Li<sup>1†</sup>, Chenglong Zheng<sup>1†</sup>, Jingyu Liu<sup>2</sup>, Guocui Wang<sup>2, 3</sup>, Hang Xu<sup>1</sup>, Mingyang Chen<sup>4</sup>, Yating Zhang<sup>1\*</sup>, Yan Zhang<sup>2\*</sup> and Jianquan Yao<sup>1\*</sup>

<sup>1</sup>Key Laboratory of Opto-Electronics Information Technology (Tianjin University), Ministry of Education, School of Precision Instruments and Opto-Electronics Engineering, Tianjin University, Tianjin 300072, China; <sup>2</sup>Beijing Key Laboratory for Metamaterials and Devices, Department of Physics, Capital Normal University, Beijing 100048, China; <sup>3</sup>Beijing Engineering Research Center for Mixed Reality and Advanced Display, School of Optics and Photonics, Beijing Institute of Technology, Beijing 100081, China; <sup>4</sup>Department of Optoelectronic Information Science and Engineering, Jiangsu University, Zhenjiang 212013, China.

<sup>†</sup>These authors contributed equally to this work.

\*Correspondence: YT Zhang, E-mail: [yating@tju.edu.cn](mailto:yating@tju.edu.cn); Y Zhang, E-mail: [y Zhang@cnu.edu.cn](mailto:y Zhang@cnu.edu.cn); JQ Yao, E-mail: [jyao@tju.edu.cn](mailto:jyao@tju.edu.cn)

## This file includes:

[Section 1: Derivation of Fresnel zone theory](#)

[Section 2: Derivation of the metasurface zone plate](#)

[Section 3: Meta-atoms applied to the linear polarizer](#)

[Section 4: Sample fabrication](#)

Supplementary information for this paper is available at <https://doi.org/10.29026/oes.2022.210014>



**Open Access** This article is licensed under a Creative Commons Attribution 4.0 International License.

To view a copy of this license, visit <http://creativecommons.org/licenses/by/4.0/>.

© The Author(s) 2022. Published by Institute of Optics and Electronics, Chinese Academy of Sciences.

### Section 1: Derivation of Fresnel zone theory

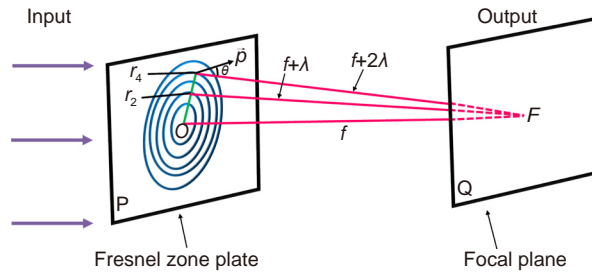


**Fig. S1 | Schematic diagram of the Fresnel zone theory.**

As depicted in Fig. S1, when a parallel beam with wavelength of  $\lambda_0$  is incident on the Fresnel zone plate, the outgoing beam will be focused on the point (F) which is away from the zone plate by  $f$ . The zone plate is composed of a series of concentric rings with the center at the point (O), and the outer radius of the  $n$ th ring is  $r_n$  ( $n$  is a positive integer). Meanwhile, the distance from any point on the  $n$ th concentric circle to the focus can be expressed as:  $d_n = f + n\lambda_0/2$ . Therefore, it can be judged that the exit waves of adjacent ring zones exist a phase difference of  $\pi$  at the focus.

Let us discuss the amplitude of the outgoing beam generated by the Fresnel zone plate at the focus. According to the Huygens-Fresnel theory, the amplitude (at the focus) of exit beam responses to the  $n$ th ring zone can be expressed as:

$$|\mathbf{E}_n| = K \cdot \frac{S_n}{d_n} \cdot \frac{1 + \cos\theta}{2}, \tag{S1}$$

where  $K$  is a proportional constant,  $(1 + \cos\theta)/2$  represents the tilt factor related to angle  $\theta$ , and  $S_n$  stands for the area of the  $n$ th ring zone. As seen from Fig. S1,  $r_n$  can be written as:

$$r_n = \sqrt{d_n^2 - f^2} = \sqrt{nf\lambda_0} \left(1 + \frac{n\lambda_0}{4f}\right)^{1/2}, \tag{S2}$$

and then the corresponding area  $S_n$  of ring zone is:

$$S_n = \pi r_n^2 - \pi r_{n-1}^2 = \pi f \lambda_0 + \frac{2n-1}{4} \pi \lambda_0^2. \tag{S3}$$

Substituting Eq. (S3) into Eq. (S1) can be obtained as follows:

$$|\mathbf{E}_n| = K \cdot \left( \pi f \lambda_0 + \frac{2n-1}{4} \pi \lambda_0^2 \right) \cdot \frac{1 + \cos\theta}{2(f + n\lambda_0/2)}. \tag{S4}$$

After obtaining the derivative of Eq. (S4), it can be determined that once  $f$  is much larger than  $\lambda_0$ , the amplitude  $|\mathbf{E}_n|$  decreases monotonously and changes slowly as  $n$  increases. Besides, when the value of  $n$  is small, it can be considered that  $|\mathbf{E}_n|$  is approximately equal to  $|\mathbf{E}_1|$ . Thus, the complex amplitude of the exit wave generated by the zone plate at focus is:

$$\mathbf{E} = \sum_{i=1}^n \mathbf{E}_i = \begin{cases} \mathbf{E}_1, & n = 1 \\ \sum_{j=1}^m \mathbf{E}_{2j-1} + \sum_{j=1}^{m-1} \mathbf{E}_{2j}, & n = 2m - 1 \\ \sum_{j=1}^m \mathbf{E}_{2j-1} + \sum_{j=1}^m \mathbf{E}_{2j}, & n = 2m \end{cases} \approx \begin{cases} |\mathbf{E}_1|, & n = 1 \\ m |\mathbf{E}_1| + e^{i\pi} (m-1) |\mathbf{E}_1|, & n = 2m - 1 \\ m |\mathbf{E}_1| + e^{i\pi} m |\mathbf{E}_1|, & n = 2m \end{cases}, \tag{S5}$$

here,  $m$  is a positive integer greater than 1.

### Section 2: Derivation of the metasurface zone plate

Each ring zone of the metasurface zone plate can be composed of different microstructured dielectric pillars, so each ring zone can have different functions, which enriches the versatility of the zone plate. Here, we only consider the case where odd-numbered and the even-numbered ring zones have different functions. When a lossless anisotropy element

atom rotates  $\theta$  along the optical axis, the corresponding transmission coefficient can be represented by the Jones matrix:

$$\mathbf{J} = \mathbf{R}^T \begin{bmatrix} e^{i\varphi_x} & 0 \\ 0 & e^{i\varphi_y} \end{bmatrix} \mathbf{R} = \begin{bmatrix} \cos\theta & -\sin\theta \\ \sin\theta & \cos\theta \end{bmatrix} \begin{bmatrix} e^{i\varphi_x} & 0 \\ 0 & e^{i\varphi_y} \end{bmatrix} \begin{bmatrix} \cos\theta & \sin\theta \\ -\sin\theta & \cos\theta \end{bmatrix}, \quad (\text{S6})$$

where  $\mathbf{R}$  represents rotation matrix,  $\varphi_x$  is the phase delay propagating along the  $x$  direction under  $x$ -LP incidence, while  $\varphi_y$  stands for the corresponding phase delay under  $y$ -LP incidence. For RCP ( $[1 \ i]^T$ ) incidence, the transmitted electric field is<sup>1</sup>:

$$\mathbf{E}_{\text{out1}} = \cos\left(\frac{\Delta\varphi}{2}\right) \cdot e^{i\frac{\Sigma\varphi}{2}} \cdot \begin{bmatrix} 1 \\ i \end{bmatrix} + \sin\left(\frac{\Delta\varphi}{2}\right) \cdot e^{i(\frac{\Sigma\varphi}{2} - \frac{\pi}{2} + 2\theta)} \cdot \begin{bmatrix} 1 \\ -i \end{bmatrix}. \quad (\text{S7})$$

where  $\Sigma\varphi$  is the summation of phases  $\varphi_x$  and  $\varphi_y$ , and the phase difference between phases  $\varphi_x$  and  $\varphi_y$  is described as  $\Delta\varphi = \varphi_x - \varphi_y$ . Similarly, the transmitted electric field under LCP incidence can be expressed as:

$$\mathbf{E}_{\text{out2}} = \cos\left(\frac{\Delta\varphi}{2}\right) \cdot e^{i\frac{\Sigma\varphi}{2}} \cdot \begin{bmatrix} 1 \\ -i \end{bmatrix} + \sin\left(\frac{\Delta\varphi}{2}\right) \cdot e^{i(\frac{\Sigma\varphi}{2} - \frac{\pi}{2} - 2\theta)} \cdot \begin{bmatrix} 1 \\ i \end{bmatrix}. \quad (\text{S8})$$

It is supposed that the meta-atoms in the even-numbered ring zones are the same, and the meta-atoms that construct the odd-numbered ring zones are the same. For the incident beam  $\mathbf{E}_{\text{in}}$  with an amplitude of 1, combining Eqs. (4), (S5) (S7) and (S8), the transmitted fields generated by the even-numbered and odd-numbered ring zones at the focus can be obtained:

$$\begin{aligned} \mathbf{E}_{\text{oute}} &= \left[ \frac{A - iB}{4} \cdot \cos\left(\frac{\Delta\varphi_1}{2}\right) \cdot e^{i\frac{\Sigma\varphi_1}{2}} + \frac{A + iB}{4} \cdot \sin\left(\frac{\Delta\varphi_1}{2}\right) \cdot e^{i(\frac{\Sigma\varphi_1}{2} - \frac{\pi}{2} - 2\theta_1)} \right] \cdot \begin{bmatrix} 1 \\ i \end{bmatrix} \\ &+ \left[ \frac{A - iB}{4} \cdot \sin\left(\frac{\Delta\varphi_1}{2}\right) \cdot e^{i(\frac{\Sigma\varphi_1}{2} - \frac{\pi}{2} + 2\theta_1)} + \frac{A + iB}{4} \cos\left(\frac{\Delta\varphi_1}{2}\right) \cdot e^{i\frac{\Sigma\varphi_1}{2}} \right] \cdot \begin{bmatrix} 1 \\ -i \end{bmatrix} \\ \mathbf{E}_{\text{outo}} &= \left[ \frac{iB - A}{4} \cdot \cos\left(\frac{\Delta\varphi_2}{2}\right) \cdot e^{i\frac{\Sigma\varphi_2}{2}} - \frac{A + iB}{4} \cdot \sin\left(\frac{\Delta\varphi_2}{2}\right) \cdot e^{i(\frac{\Sigma\varphi_2}{2} - \frac{\pi}{2} - 2\theta_2)} \right] \cdot \begin{bmatrix} 1 \\ i \end{bmatrix} \\ &- \left[ \frac{A - iB}{4} \cdot \sin\left(\frac{\Delta\varphi_2}{2}\right) \cdot e^{i(\frac{\Sigma\varphi_2}{2} - \frac{\pi}{2} + 2\theta_2)} + \frac{A + iB}{4} \cos\left(\frac{\Delta\varphi_2}{2}\right) \cdot e^{i\frac{\Sigma\varphi_2}{2}} \right] \cdot \begin{bmatrix} 1 \\ -i \end{bmatrix}. \quad (\text{S9}) \end{aligned}$$

where  $\Delta\varphi_1$  ( $\Delta\varphi_2$ ) is the phase difference between the orthogonal linear polarizations engendered by the even-numbered (odd-numbered) ring zones,  $\Sigma\varphi_1$  and  $\Sigma\varphi_2$  are the summation of the corresponding phase delays, and  $\theta_1$  and  $\theta_2$  are the rotation angles of the two kinds of meta-atoms.

## Section 3: Meta-atoms applied to the linear polarizer

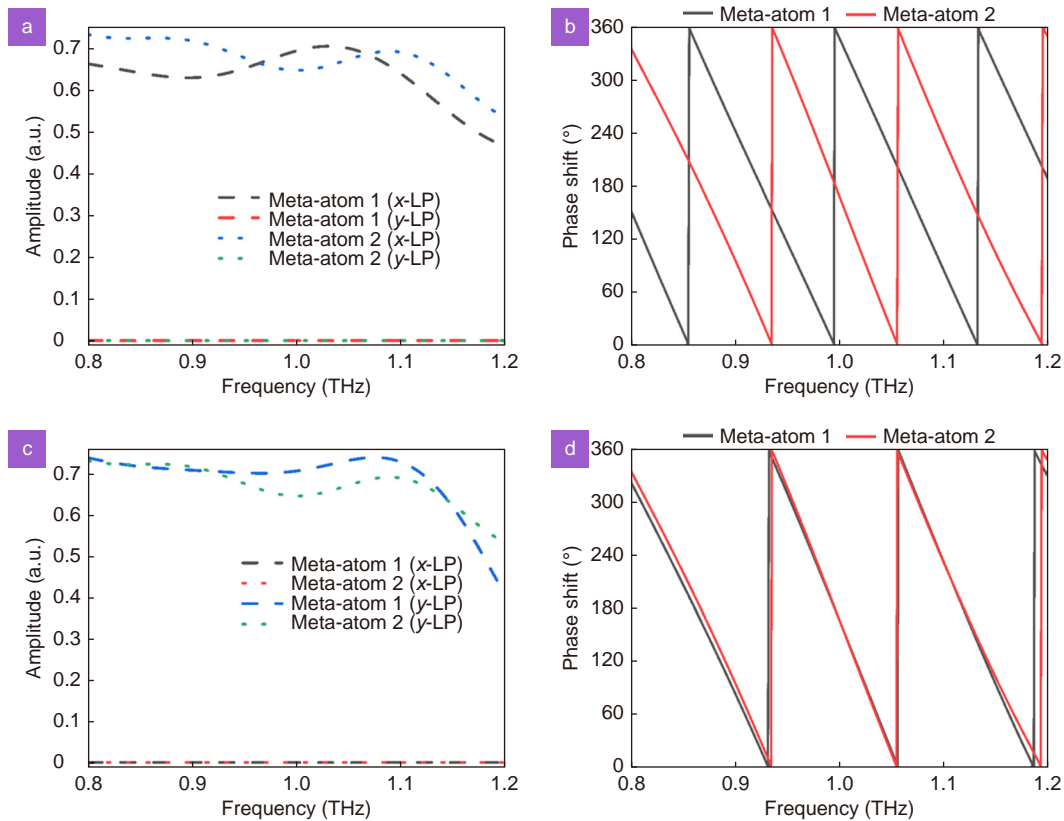


**Fig. S2** | (a, c) Transmission amplitude of Meta-atom 1 and Meta-atom 2 at different frequencies, under LP incidences. (b, d) Simulated the phase shifts of the transmitted co-polarized components under x-LP and y-LP illuminations.

Same as the previous work<sup>2-4</sup>, the transmission coefficient under orthogonal LP incidence is acquired by parametric scanning, including the transmission amplitude and phase shift. We define the basic units for constructing even-numbered and odd-numbered ring zones in Section *Linear polarizer with focusing function* as Meta-atom 1 and Meta-atom 2, respectively. Figure S2(a, c) shows the transmission amplitudes of the orthogonal LP waves generated by the two meta-atoms under x-LP (y-LP) incidence. It can be seen that under LP incidence, the outgoing waves generated by the Meta-atom 1 and Meta-atom 2 are co-polarized components at 1 THz. Figure S2(b) plots the phase shift of the co-polarized component in response to x-LP incidence at different incident frequencies. It is worth noting that the phase difference of the phase shifts generated by these two meta-atoms at 1 THz is  $\pi$ . In addition, under y-LP incidence, the phase shifts of the Meta-atom 1 and Meta-atom 2 at 1 THz are equal (see Fig. S2(d)). Since the optical path difference between the adjacent ring zone of the metasurface zone plate and the focus is  $\lambda_0/2$ , the y-LP component engendered by the odd-numbered zone and the even-numbered zone will interfere destructively while the x-LP component will interfere constructively.

## Section 4: Sample fabrication

All samples are formed by etching on high-resistance silicon ( $\epsilon = 11.9$ ) with a thickness of 150  $\mu\text{m}$  and a size of 1.4 mm $\times$ 1.4 mm. Here, standard ultraviolet lithography and inductively coupled plasma etching techniques are used to generate the metasurface zone plate. After spin-coating a positive photoresist (AZ4620) on the cleaned silicon wafer, a patterned photoresist is generated through standard ultraviolet lithography technology and used as the mask. Next, we use the (ICP) etching technique to etch the silicon wafer, and the corresponding etching depth is 200  $\mu\text{m}$ . After removing the excess photoresist, the sample with a substrate thickness of 300  $\mu\text{m}$  can be finally obtained.

## References

1. Yuan YY, Sun S, Chen Y, Zhang K, Ding XM et al. A fully phase-modulated metasurface as an energy-controllable circular polarization router. *Adv Sci* **7**, 2001437 (2020).
2. Yue Z, Liu JY, Li JT, Li J, Zheng CL et al. Multifunctional terahertz metasurfaces for polarization transformation and wavefront manipulation. *Nanoscale* **13**, 14490–14496 (2021).
3. Cai XD, Tang R, Zhou HY, Li QS, Ma SJ et al. Dynamically controlling terahertz wavefronts with cascaded metasurfaces. *Adv Photonics* **3**, 036003 (2021).
4. Wang DY, Liu FF, Liu T, Sun SL, He Q et al. Efficient generation of complex vectorial optical fields with metasurfaces. *Light Sci Appl* **10**, 67 (2021).